New Journal of Physics
An Institute of Physics and Deutsche Physikalische Gesellschaft Journal

Comparison of turbulence measurements and simulations of the low-temperature plasma in the torsatron TJ-K

C Lechte[1], **S Niedner**[1,2] **and U Stroth**[1]

[1] IEAP, University of Kiel, 24098 Kiel, Germany
[2] MPI für Plasmaphysik, EURATOM Association, Garching, Germany
E-mail: stroth@physik.uni-kiel.de

New Journal of Physics **4** (2002) 34.1–34.16 (http://www.njp.org/)
Received 22 April 2002, in final form 16 May 2002
Published 21 June 2002

Abstract. A toroidal low-temperature plasma is used for comparative turbulence studies. Measurements are carried out with Langmuir probe arrays in the entire plasma cross section. The data are closely compared with drift-Alfvén turbulence simulations. Although the parameters in a low-temperature plasma are very different from those in fusion plasmas, the dimensionless parameters governing the drift-wave physics are comparable. Hence this study can also give insight into high-temperature plasma turbulence. In order to identify relevant characteristic signatures of different turbulence-driving mechanisms, simulations were carried out for a wide range of plasma parameters. The simulation results are compared with first measurements.

1. Introduction

Turbulence is considered to be one of the most interesting problems in modern physics. It has been studied in fluids for five centuries and still is an active field of research [1, 2]. In magnetized plasmas the problem is even more severe. The Navier–Stokes equation for fluids has to be replaced by magneto-hydrodynamic equations for the electron and ion fluids which couple to Maxwells equations. In the presence of a guiding magnetic field, the turbulence can change from that of a two-dimensional to a three-dimensional system. Fluctuations in a plasma are not restricted to the density. For a full description, temperature, potential and magnetic field fluctuations have to be taken into account.

The interest in plasma turbulence was strongly stimulated by fusion research. Turbulence is responsible for most of the detrimental particle and energy losses of fusion plasmas. However, the diagnostics of turbulence in high-temperature fusion plasmas is rather restricted. Therefore,

1367-2630/02/000034+16$30.00

most data are available from the plasma edge or from plasmas with reduced parameters. The first extensive studies were carried out in the 1980s on small and medium sized tokamaks. A review of the early experiments and comparisons with linear turbulence models can be found in [3] and for more recent data see [4].

Since then progress has been made in the measurement of the microscopic features of the turbulent eddies. By means of correlation techniques, the spatial structure of the micro-fluctuations perpendicular and parallel to the magnetic field were measured in the scrape-off layer (SOL) of stellarators and tokamaks [5, 6]. The results are consistent with predictions from electrostatic interchange turbulence. The statistical properties of data from different devices where compared [7, 8] and more sophisticated methods were applied to learn about the relevance of concepts such as self-organized criticality, intermittency, self-similarity [9] or zonal flows driven by Reynolds stress [10, 11] through three-wave interaction [12]–[14]. The data for these studies are measured by probes, which only can access the edge of high-temperature plasmas. For the investigation of core turbulence much more technical effort is needed. Beam emission spectroscopy [15] and heavy ion beam probes [16] are examples.

As in other fields of physics, a close comparison between theoretical turbulence simulations and measurements would be needed. Due to improved computer performance the theoretical investigation of turbulence has progressed considerably [17, 18]. The simulation of turbulence in a large plasma volume [19] and in realistic magnetic geometry [20] has become possible. Nevertheless, the effort to compare experiment and theory directly has, until now, been rather limited.

In order to test the physical models behind the simulations as well as the data analysis techniques, simultaneous *measurements* of plasma potential, density and temperature fluctuations with high spatial and temporal resolution from both the experimental and the simulated plasma is needed. It would be desirable to process both sets of data with the same analysis software. From turbulence simulation codes these data are readily available. In real plasmas probes are the best diagnostic to obtain the full information. In fusion plasmas, probe measurements can be carried out in the open flux geometry of the SOL. Due to direct wall contact and limited connection lengths, this area might not be representative for the confinement region. One way to extend the measurements to the core is to use toroidally confined low-temperature plasmas. This approach is pursued in this paper.

Low-temperature plasmas in linear devices have already been exploited to investigate the initial transition from drift waves with a few mode numbers to a turbulent state [21]. In order to study fully developed turbulence on closed magnetic surfaces without direct wall contact, a toroidal device has to be used. The best configuration to maintain a toroidal low-temperature plasma under stationary conditions is a stellarator. This paper reports on such an experiment. The torsatron TJ-K confines an MHD stable toroidal plasma. The low-temperature plasma allows for Langmuir probe access in the entire plasma cross section. The experiment is accompanied by turbulence simulations performed with the drift-Alfvén turbulence code DALF3 [22], which was originally designed for the fusion SOL. Simulations were carried out at the TJ-K plasma parameters and compared with first experimental results. The paper also intends to demonstrate that results from low-temperature plasmas are also relevant for fusion plasmas.

The paper is organized as follows. The next section introduces the TJ-K experiment. Section 3 summarizes the simulation results and section 4 gives the first experimental results and the comparison. The comparison is summarized and discussed in section 5.

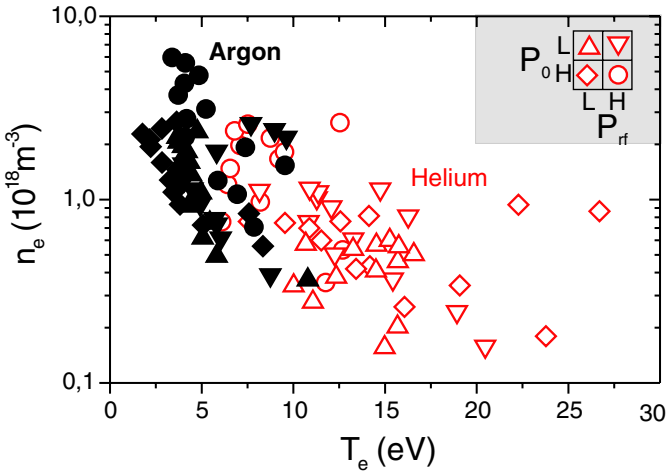

Figure 1. Typical plasma parameters (density from interferometry, temperature from swept Langmuir probes) for helium (open symbols) and argon (solid) for low (10^{-4}) and high (10^{-3} mbar) neutral gas pressure P_0 and low (1) and high (3 kW) heating power p_{rf}. For each parameter set, the magnetic field was varied from 50 to 200 mT.

2. The torsatron TJ-K

TJ-K is an $l = 1$, $m = 6$ torsatron [23, 24]. Minor and major plasma radii are 0.1 and 0.6 m, respectively, the magnetic field strength is $B \leq 0.3$ T and the rotational transform (ι) is about $1/3$. The magnetic field configuration can be varied to a large extent. This allows one to study the influence of magnetic shear, magnetic well, ι and rational surfaces on turbulence.

Discharge durations up to 60 min are possible. The plasma is created by rf heating at 27.12 MHz and powers up to $p_{rf} = 3$ kW. In this range helicon waves propagate in the plasma. The working gases are hydrogen, helium and argon at a neutral gas pressure P_0 of typically 10^{-4}–10^{-3} mbar. The achieved densities are up to $n_e = 6 \times 10^{18}$ m^{-3} and the electron temperatures up to $T_e = 30$ eV. The ions are cold.

The range of accessible plasma parameters as measured by an interferometer and swept Langmuir probes is shown figure 1. The scatter in the data is due to variations in B, p_{rf} and P_0. A comparison with a combined particle and power balance analysis can be found in [25]. Argon plasmas reside at higher densities and lower temperatures than helium plasmas. Hydrogen plasmas, which have not yet been investigated in depth, tend to even lower density and higher temperature. The highest densities are achieved at highest heating power and highest neutral gas pressure.

For turbulence studies a movable Langmuir probe array is used, which can be scanned through the entire plasma cross section. Figure 2 depicts a measured two-dimensional density profile. It consists of 200 independent local measurements of the ion saturation current carried out during 10 min in a single discharge. The result demonstrates the stationarity of the plasma conditions and, since for the high-field-side points the probe pierces the plasma from the low-field side, the limited distortion of the plasma by the probes. The profile is radially peaked and it reflects the shape of the overlaid flux surfaces, which are triangular at this toroidal position. The probe array enters through the port on the left-hand side.

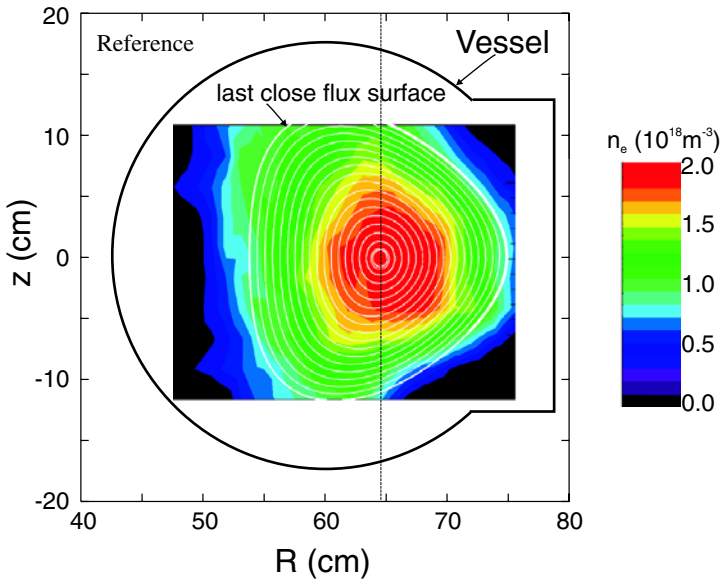

Figure 2. Two-dimensional poloidal density profile (from saturation current) in the poloidal cross section. The parameters are $B = 0.09$ T, $p_{rf} = 3$ kW, $T_e \approx 13$ eV in helium at 10^{-4} mbar. Flux surfaces calculated with the Gourdon code are overlaid. The cross section of the vacuum vessel and port through which the movable probe enters is indicated by the solid line.

3. Numerical turbulence simulations

For comparison with experimental data, turbulence simulations were carried out using the drift-Alfvén code DALF3 [22, 26]. It solves the two fluid equations in the drift approximation. The background gradients are kept fixed. The simulations are performed in equivalent tokamak geometry at the plasma parameters measured in TJ-K. The strong variations of local shear and curvature introduced by the helical coil are not yet included. The investigation of the influence of local shear on turbulence is an especially interesting topic [27] left for future investigations. The effect of trapped particles can only be taken into account through an effective collisionality.

The code includes curvature-driven as well as drift-wave instabilities. Hence it covers the whole range from interchange, resistive ballooning to drift-wave turbulence. The parallel dynamics of the drift wave is coupled to torsional Alfvén waves. Temperature gradient driven modes are not included. Temperature fluctuations are neglected and the ions are treated as cold, which is consistent for the plasma of interest. The equations solved in DALF3 have the form [22]:

$$\frac{nM_ic^2}{B^2}\left(\frac{\partial}{\partial t}+\boldsymbol{v}\cdot\nabla\right)\nabla_\perp^2\phi=\nabla_\parallel J_\parallel+\nabla\cdot\frac{c}{B^2}\boldsymbol{B}\times\nabla p_e \tag{1}$$

$$\frac{ne}{c}\frac{\partial}{\partial t}A_\parallel+\frac{m_e}{e}\left(\frac{\partial}{\partial t}+\boldsymbol{v}\cdot\nabla\right)J_\parallel=\nabla_\parallel p-ne\nabla_\parallel\phi-0.51\frac{m_e}{e}\nu_eJ_\parallel \tag{2}$$

$$\left(\frac{\partial}{\partial t}+\boldsymbol{v}\cdot\nabla\right)p_e=\gamma\frac{p_e}{ne}\nabla_\parallel J_\parallel-\gamma p\nabla_\parallel u_\parallel, \tag{3}$$

$$v_\parallel=u_\parallel-\frac{J_\parallel}{n_ee}. \tag{4}$$

It consists of charge conservation (1), the parallel electron momentum equation (2) and the energy equation (3). The electrostatic and parallel vector potentials are denoted by ϕ and $A_\parallel$, respectively. The collision rate is ν_e, and m_e, p_e and e denote the electron mass, the electron pressure and the electron charge. M_i is the ion mass, $\boldsymbol{u}$ and $\boldsymbol{v}$ are the ion and electron flow velocities, and γ is the ratio of specific heats. Electric and magnetic field fluctuations are coupled by the Maxwell equations.

Solutions are obtained on closed flux tubes with periodic boundary conditions. The flux tube closes after three toroidal turns ($\iota = 1/3$) and therefore includes regions of good and bad curvature. It is divided into a grid typically with 128×64 points in the perpendicular plane, where 64 points are in the direction of the density gradient. The direction along the magnetic field is resolved by 16 points. Throughout this paper, we will compare the dynamics in the perpendicular plane with the dynamics in a poloidal cross section of the plasma. These two planes are slightly tilted due to the rotational transform. This can be neglected due to the fast parallel dynamics.

The dynamics of electron and ion fluids is governed by three dimensionless parameters. They fully determine the character of the turbulence. In order to compare the results with data from plasmas at different parameters, the absolute values of these parameters are important. They are defined as follows.

The *collisionality* is the electron–electron collision frequency ν_{ee} normalized to the velocity of sound c_s over the density gradient length $L_\perp$,

$$\hat{\nu} = \frac{\nu_{ee} L_\perp}{c_s}. \tag{5}$$

It mainly determines the parallel electron dynamics and therefore the instability of the drift wave. The electron *plasma* β is normalized to the ratio of parallel connection length $L_\parallel = R/\iota$ and $L_\perp$,

$$\hat{\beta} = \frac{\beta_e}{2}\left(\frac{R}{\iota L_\perp}\right)^2. \tag{6}$$

This parameter drives the interchange instability. Finally enters the ratio of the timescales of the parallel to perpendicular dynamics which is represented by the electron–ion mass ratio,

$$\hat{\mu} = \frac{m_e}{m_i}\left(\frac{R}{\iota L_\perp}\right)^2. \tag{7}$$

In order to map the turbulent eddies from normalized to real space, they have to be multiplied by the drift scale, which is the ion gyro radius taken at the electron temperature:

$$\rho_s = \frac{c_s}{\omega_{ci}} = \frac{\sqrt{m_i T_e}}{eB}. \tag{8}$$

Prior to a comparison of experimental data with simulations it has to be addressed whether these results are also meaningful for fusion plasmas. Primarily two elements are critical, collisionality and magnetization of the low-temperature plasma as well as the dimensionless parameters with respect to those of high-temperature plasmas.

Important, and for low-temperature plasmas, always critical conditions are collisionality and magnetization. The relevant parameters were verified for singly charged helium ions at the unfavourable parameters of $T_e = 5$ eV, $T_i = 1$ eV, $B = 0.1$ T, $n_e = 10^{18}$ m^{-3} and $P_0 = 5 \times 10^{-3}$ mbar. The parameters yield electron and ion Larmor radii of $\rho_{Le} \approx 0.01$ mm and $\rho_{Li} \approx 3$ mm, respectively. Both are small with respect to the plasma radius. The electron–electron and electron–neutral collision frequencies normalized to the electron gyro frequency

Table 1. Physical and normalized parameter sets for typical TJ-K plasmas and for the edge of fusion plasmas. $L_\parallel = 15$ m and $L_\perp = 5$ cm (8 cm for fusion edge) were used. $\hat{\mu}$ is 1.2 for hydrogen, 0.3 for helium and 0.03 for argon.

n_e (m^{-3})	T_e (eV)	B_0 (T)	Gas	$\hat{\nu}$	$\hat{\beta}$	ρ_s (cm)	
2.0×10^{19}	150	2.0	H	1	0.9	0.1	Fusion edge
3.6×10^{18}	25	0.20	He	4	1.0	0.5	$\hat{\beta}$ scan
1.8×10^{18}	18	0.17	He	4	0.5	0.5	
3.6×10^{17}	8	0.11	He	4	0.1	0.5	
6.3×10^{17}	21	0.10	He	1	0.7	1.0	$\hat{\nu}$ scan
2.5×10^{18}	21	0.20	He	4	0.7	0.5	
1.7×10^{18}	8	0.10	H	10	0.7	0.3	
3.9×10^{18}	18	0.22	H	4	0.7	0.2	ρ_s scan
1.7×10^{18}	18	0.14	He	4	0.7	0.6	
6.3×10^{17}	11	0.06	He	4	0.7	1.0	
2.5×10^{17}	12	0.04	Ar	4	0.7	5.0	

are $\approx 2 \times 10^{-4}$ and ≈ 0.02, respectively. For the ions both values are approximately 1.5. Hence electrons are perfectly magnetized and rather collisionless. The magnetization of the ions is marginal. The chosen parameters are, however, unfavourable and at lower density or higher magnetic field hydrogen and helium ions can be considered as magnetized. For the parameters of interest (see table 1) the parameters are more favourable throughout. For argon, however, ion–ion collisions impose a severe limit on the magnetization condition.

In table 1 the normalized parameters of typical TJ-K plasmas are compared with those of the fusion plasma edge. Although the plasma parameters are very different, the normalized parameters fall in the same range. Furthermore, scans for single parameters with the other parameters constant should be possible. For example, the scaling with ρ_s is of interest for fusion experiments for better predicting large devices [28].

Systematic numerical simulations were carried out on a large range of dimensionless parameters also covering the parameters given in table 1 [26]. The focus was on two single-parameter scans, a $\hat{\nu}$ scan ranging from 1.0 to 6.0 at $\hat{\beta} = 0.7$ and a $\hat{\beta}$ scan ranging from 0.5 to 4.25 at $\hat{\nu} = 4.0$. The objective was to identify meaningful quantities for a comparison with experiment and their scaling properties.

First simple parameters were evaluated, such as the relative levels of density $\tilde{n}/n$ and potential $e\tilde{\phi}/T_e$ fluctuations. The scaling of these parameters can be found in figure 3. In the low $\hat{\nu}$, low $\hat{\beta}$ regime relevant for the comparison, fluctuation amplitudes of 20% can be expected. The amplitudes increase with both $\hat{\beta}$ and $\hat{\nu}$. The Boltzmann relation is fulfilled. Only at the highest $\hat{\beta}$ values, do the density fluctuations become larger than the potential fluctuations. The ballooning structure can be seen in the density and but not in the potential fluctuations. Since the turbulence does not act back on the background gradient (local model), especially at large fluctuation amplitudes the values produced by the code probably overestimate the actual fluctuation level.

Since the background $E \times B$ plasma rotation is not taken into account in the simulations, the direct comparison of frequency spectra cannot be relied on very much. Wavenumber spectra

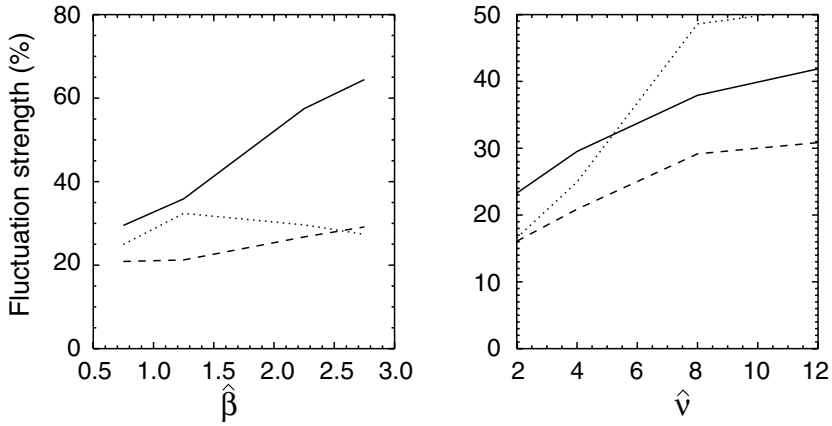

Figure 3. Relative density fluctuation amplitudes from the low- (continuous) and high-field sides (dashed) and potential fluctuation amplitudes (dotted curve), which do not share the ballooning structure of the density fluctuations. Note that these figures have been obtained for helium and not for hydrogen as the rest of the figures in this section (different $\hat{\mu}$.)

should be measured in the future. Simulations have the advantage that wavenumber spectra can be readily calculated. In figure 4 the poloidal wavenumber spectra of density and $\tilde{E} \times B$ transport fluctuations for the two scans are depicted. The change in collisionality leaves the density fluctuation spectrum almost unchanged. At the same time transport increases. The spectrum of turbulent transport is rather flat with strong contributions in the region where the density fluctuation amplitude already decays exponentially. This difference between the density and transport spectrum is not due to the potential fluctuation amplitude but due to large cross phases between the density and potential fluctuations.

As $\hat{\beta}$ increases, more and more energy goes into the small wavenumbers. Both density and transport spectra pass over into a peaked shape. The strongest change is due to large-scale modes. The largest $\hat{\beta}$ is, however, far beyond the accessible range of TJ-K.

The cross phase between the density and potential fluctuations has turned out to be a sensitive quantity to disentangle the turbulence driving mechanisms [22, 26]. This is demonstrated in figure 5 where poloidal wavenumber resolved cross-phase spectra are depicted. In order to demonstrate the different signatures of drift wave and interchange turbulence in this representation, two idealized simulations were carried out and compared with a realistic one at TJ-K parameters and a high-$\hat{\beta}$ run. The results are shown in figure 5.

In run (i), where the parallel electron dynamics was artificially switched off, the turbulence is driven by curvature. In this case cross phases of $\pi/2$ are found for all wavelengths. This is a typical signature of MHD-like turbulence which has a two-dimensional structure. In the pure drift-wave case (ii), where the magnetic inhomogeneities were neglected but the parallel electron dynamics taken into account, the phases are approximately zero. At low resistivity this reflects the adiabatic response of the electrons to the parallel density gradient. Simulations with the full code and for realistic TJ-K parameters (iii) clearly exhibit a drift-wave like behaviour. This is true for the entire accessible parameter range of TJ-K. The phase is largest at intermediate frequencies and increases slowly with resistivity. Furthermore, the spectra become broader [26]. This result explains the shape and scaling properties of the transport spectrum discussed above. In a run at

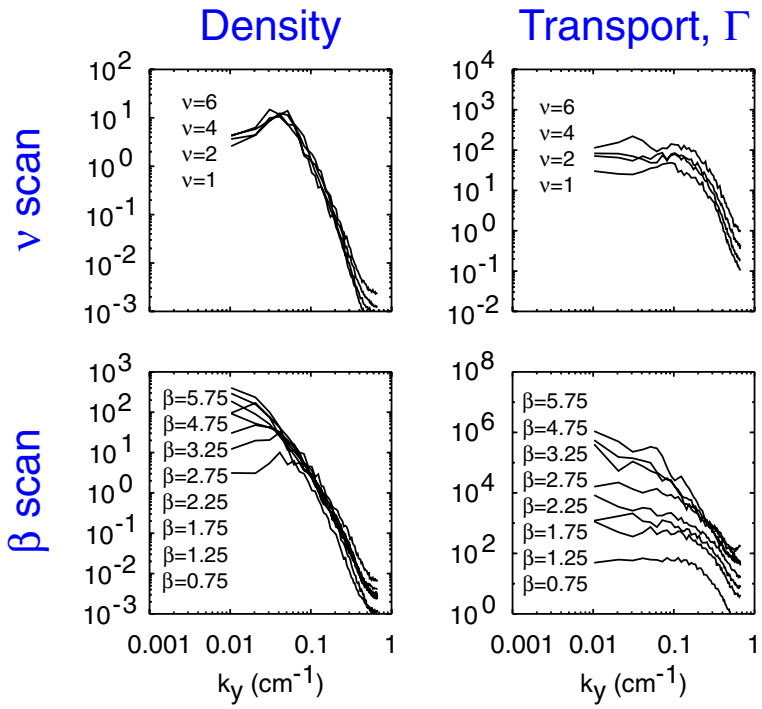

Figure 4. Poloidal wavenumber spectra of density (left) and transport fluctuations (right) for the $\hat{\nu}$ (top) and the $\hat{\beta}$ scan (bottom).

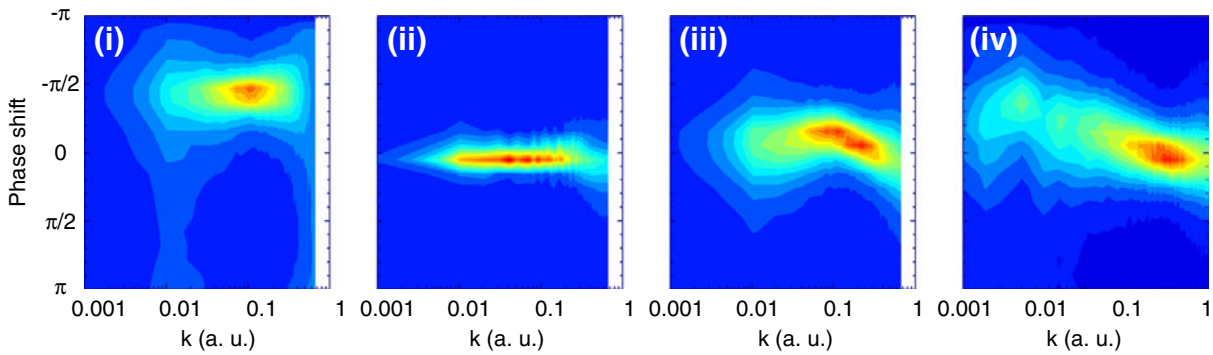

Figure 5. Poloidal wavenumber resolved density–potential cross-phase spectra for MHD turbulence (i), pure drift-wave turbulence (ii), for typical TJ-K parameters with both mechanisms active (iii) and for a high $\hat{\beta}$ case (iv), where the MHD feature shows up at long wavelengths.

high $\hat{\beta}$ values with the full code (IV) the MHD signature shows up at the long-wavelength end of the spectrum. These parameters are unrealistic for TJ-K plasmas.

Besides this spectral information, correlation and conditional averaging techniques were also applied to the simulation data. Results will be quoted in the next section. Studies to test the capability of more advanced analysis techniques such as wavelet [29] or bispectral analyses [12, 13] are under way.

4. Turbulence measurements and comparisons

Turbulence measurements in TJ-K were carried out in helium and argon plasmas. The data presented here together with simulation results were achieved at the parameters $B = 0.09$ T, $p_{rf} = 3$ kW in helium at $P_0 = 10^{-4}$ mbar. The central electron temperature was about 13 eV and the density 6×10^{17} m^{-3}. The simulations were carried out for the same plasma parameters, i.e. $\hat{\nu} = 4.0$, (the actual value from the normalization is lower, it has been raised to reflect the effects of Landau damping) $\hat{\beta} = 0.75$ and $\hat{\mu} = 0.3$. The drift scale is $\rho_s = 1.0$ cm.

As a first simple estimate the density fluctuation amplitudes were compared with values estimated from the mixing length argument: $\tilde{n}/n = 1/kL_n$. The poloidal size of the eddies d as measured by correlation techniques was used to calculate the wavenumber as $k \approx 2\pi/d$. In figure 6 the data are put in context with earlier results from various devices [3]. The density fluctuation amplitudes measured in TJ-K are consistent with mixing length estimates. For the discharge investigated here, the average fluctuation amplitudes were $\tilde{n}/n \approx 12\%$ and $e\tilde{\phi}/T \approx 10\%$; from the simulation values of about 20% can be expected (see figure 3).

As shown in figure 7, the fluctuation amplitude changes with radius. The change can be roughly expressed as a density scaling as $1/n$. This is a robust feature also known from stellarators and tokamak fusion devices [30]. This similarity points to the similar nature of the turbulence in both types of plasmas.

Although experimental frequency spectra are modified by $E \times B$ background flows, a comparison with simulated spectra is instructive. Figure 8 shows density and transport fluctuation spectra and probability density functions (PDF) as calculated from experimental and simulated data. The measured spectra are typical of plasma turbulence [31]. Similarly to as in the simulation spectra a flat region up to about 10–20 kHz if followed by an exponential decay up to 300 kHz. In the experimental data, the flat region is followed by an intermediate range with an exponent of about -1, which then turns into a second range with a significantly steeper slope. Two slopes are also indicated in the simulated transport spectrum. In the simulated density spectrum, the regions of different slopes are not evident. The turbulent cascades extend over more than three

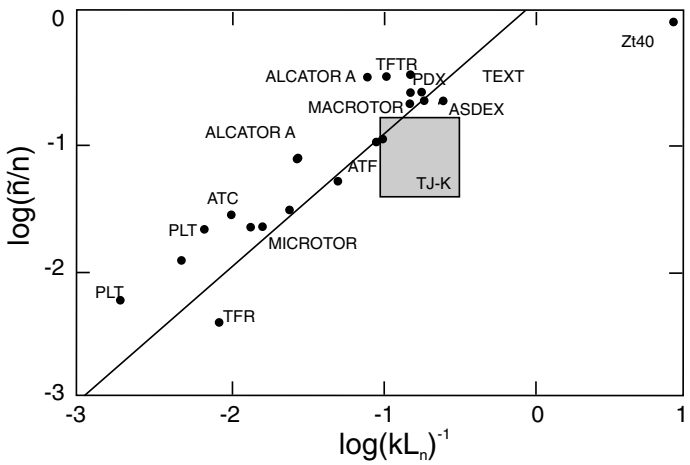

Figure 6. Relative fluctuation amplitude versus the mixing length estimate for TJ-K compared with data adapted from [3]. More recent data from ASDEX [5] were added.

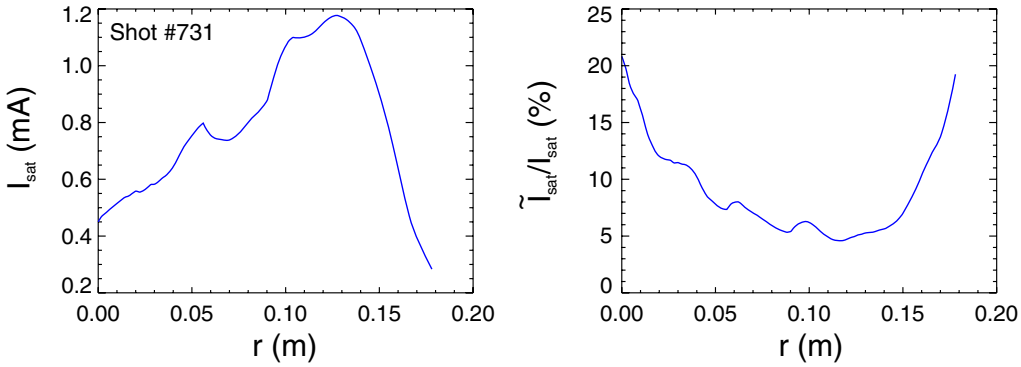

Figure 7. Radial profiles of ion saturation current and the relative fluctuation amplitude for a helium plasma at standard parameters.

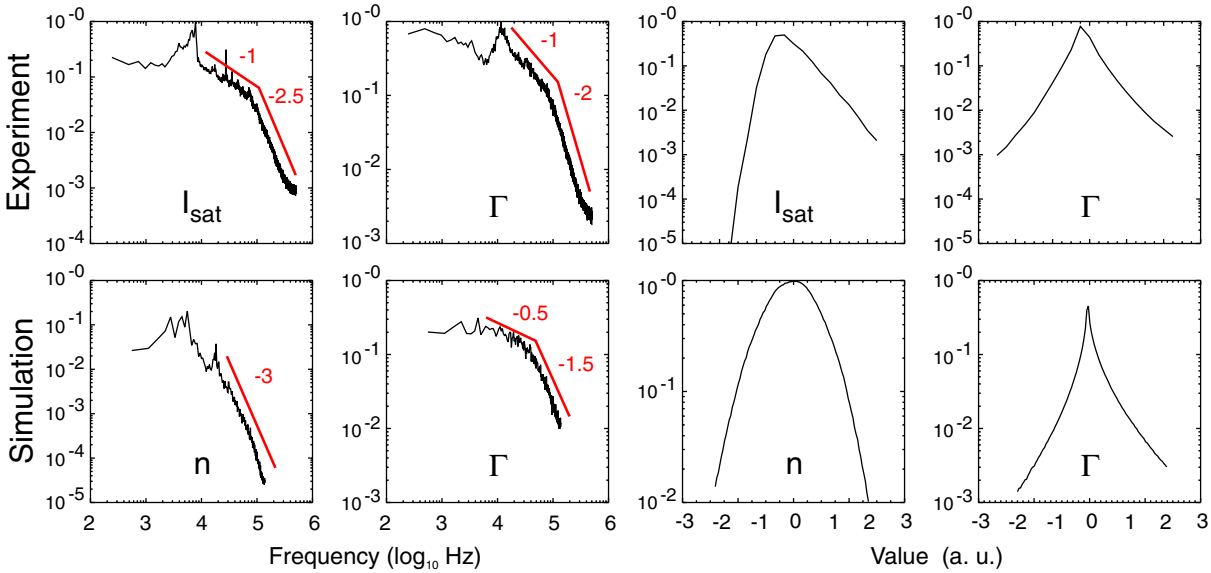

Figure 8. Comparison of measured and simulated turbulence. From left to right: power spectra of density (ion saturation current) and transport fluctuations and probability density functions (PDFs) of density (ion saturation current) and transport fluctuations. All ordinates are in arbitrary (normalized) units and are logarithmic. Experimental data is plotted in the upper row, simulation data in the lower row. The exponents for the power laws of the inertial spectral region are given in red.

decades. The slopes for the experimental spectra are similar to the simulation's. However, the experimental slopes can be modified by background flow [8] and there is a variation from discharge to discharge. In both the experimental and simulation data, individual modes are present in the spectra.

As also typically observed in fusion plasmas, [32], measured and simulated PDFs for density and potential fluctuations are near Gaussian and the transport PDF is strongly peaked and outward shifted. The ion saturation current is also slightly biased towards positive fluctuations. This could

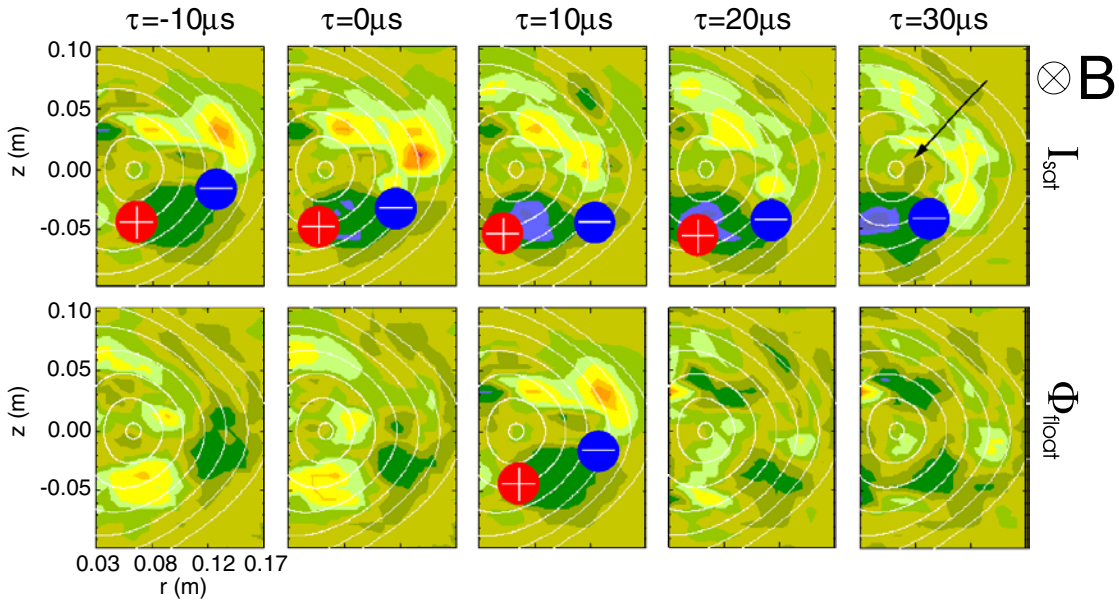

Figure 9. Correlation of the density fluctuations measured between the movable and a fixed probe array. The data was high-pass filtered at 5 kHz and then conditional averaging was applied. τ denotes the time delay introduced between the two probes. The arrow in the upper right plot gives the direction of the background radial electric field. The red and blue circles denote the positions of the floating potential maximum and minimum seen in the lower plots. A phase shift of $\pi/2$ between the density and potential is evident.

be due to the fact that the density is a positive quantity and large negative fluctuation levels are therefore limited [33]. Hence, the simple statistical features of the measured turbulence agree reasonably well with the simulation and with the properties known from high-temperature plasma turbulence. The comparison of wavenumber spectra, which will be available in the near future, will be more meaningful.

The spatial microscopic structure of the fluctuations was investigated by correlation measurements carried out with the movable probe array and spatially fixed probes mounted at a different toroidal position at a toroidal distance of about 30 cm. The density and potential fluctuations were measured simultaneously at both locations. All signals were correlated directly as well as by conditional averaging. These are methods which yield the average structure of the larger events [6, 34]. The results from both methods are consistent.

Figure 9 depicts the conditionally averaged data: the upper row shows the plasma density (ion saturation current), the lower one the plasma floating potential. The reference signal is the ion saturation current measured with the fixed probe. The condition for sampling with the movable probe was that the reference signal has a value of 1.5 standard deviations. Bright colours denote positive fluctuation amplitudes, dark colours negative fluctuations. τ indicates the time delay introduced between the reference signal and the signals from the movable probes. Hence the sequence of pictures give the average temporal evolution of the density and potential perturbations. The absolute values do not represent the value of the parallel correlation. This can only be deduced from direct correlation measurements between the probes. The values

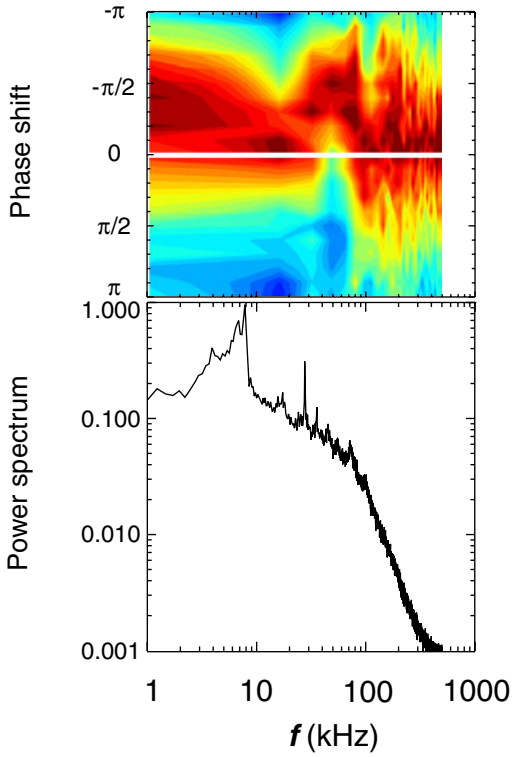

Figure 10. Frequency-resolved density–potential cross-phase spectra (top) and the corresponding density fluctuation spectrum (bottom).

are in the range from 70 to 90% for density–density, density–potential and potential–potential correlations. They are somewhat smaller than results from larger experiments [6, 35], which yielded correlations of more than 90% over a 10 m distance between probes. It has to be investigated, whether this is due to the strong local shear in TJ-K.

The 40 μs covered in figure 9 correspond to half the lifetime of the structure. A density dipole structure is visible with minimum and maximum values flanking a potential minimum, whose position seen in the lower row is copied to the ion saturation plots as circles. The potential minimum is always sandwiched between the positive and negative parts of the density dipole. Hence the phase shift between the density and potential fluctuation is about $\pi/2$ as it is typical for MHD-like instabilities.

The propagation of the dipole can be understood in terms of $E \times B$ convection. The magnetic field points into the plot and the background electric field to the plasma centre. This introduces a drift which convects the whole structure, on average, clockwise along the flux surfaces. Superimposed on that convection is an eddy motion introduced by the potential fluctuation. It increases the density amplitudes by convecting high density outward and low density inward. The low-density region can be seen to propagate counter clockwise around the potential maximum, in accordance with the $E \times B$ drift. Hence the dynamics is consistent with the linear pictures one has for MHD instabilities.

The structure seems to be a quasi-coherent mode, which can be identified in the spectrum shown in figure 10 as the rather broad peak at about 8 kHz. The average lifetime of the density structure is about 80 μs. The size of it is about 5 cm, the propagation speed of 2000 m s^{-1} is

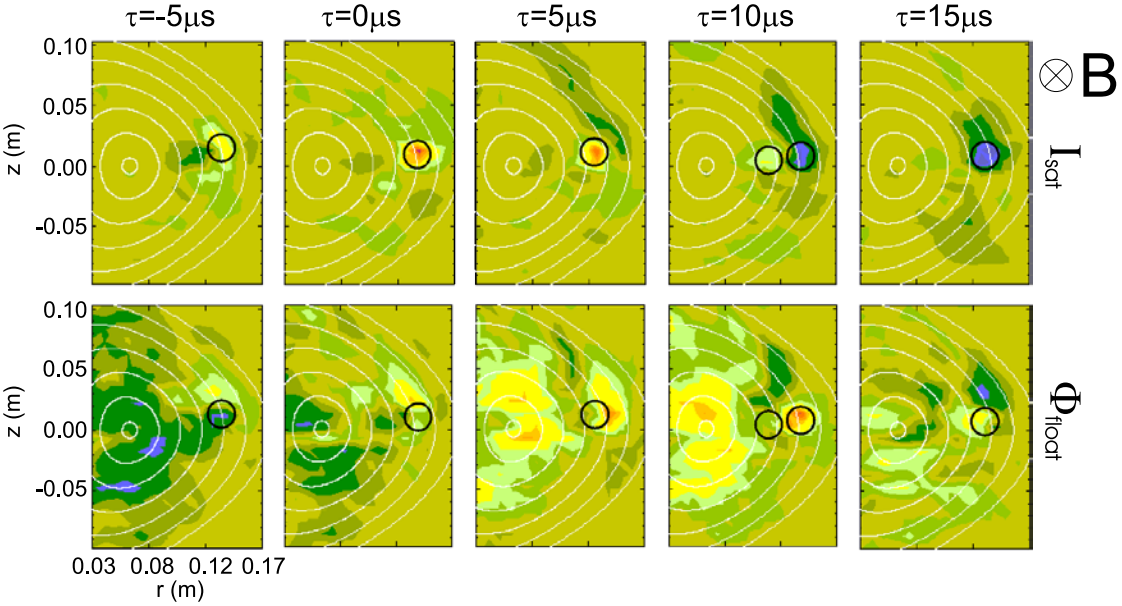

Figure 11. Same as figure 9 but with a high-pass filter at 20 kHz. The circles in the upper row are at the same position as the circles in the lower row. Here they indicate minimum (blue/dark) and maximum (red/light) density values.

consistent with the background radial electric field. A stationary probe would see a signal at 7 kHz as the density structure propagates past it. This is indeed consistent with the spectrum.

The conditional averaging technique is designed to pitch on these largest events. The quasi-coherent mode detected in figure 9 might be related to an instability at $\epsilon = 1/3$, which is inside the plasma. Such instabilities are, of course, not covered by the simulation code and it might not be representative for the broad-band turbulence responsible for the range of the spectrum with larger negative exponent.

From the numerical study drift-wave turbulence is expected for the parameters of the TJ-K plasma with a cross phase close to zero. Hence the investigation of the large structure is in variance with this prediction. In order to see whether this observation is generally valid, the cross phase was calculated as a function of the fluctuation frequency. The result is shown in figure 10. The figure at the top is a simplified version of the k spectrum, which is suggested by the simulations (see figure 5). It shows that a phase of about $-\pi/2$ is present at the frequency of the broad mode below 10 kHz in the spectrum (bottom) and also in the area of more peaks at about 30 kHz. At higher frequencies, where the background spectrum decays exponentially, the phase is around zero as expected from the simulations.

In order to access the spatio-temporal structure of the smaller scales a high-pass filter at 20 kHz was applied to the signals before they were processed by conditional averaging. The results are presented in figure 11. The density structures are now much smaller (3 cm) than for the low-frequency modes, with a shorter lifetime of about 18 μs. A positive density fluctuation can be seen propagating radially inward. It is not accompanied by a density depression—the negative density perturbation emerges only after the positive perturbation has practically decayed. Hence these fluctuations have a monopole structure. The question of the (spatial) phase between the density and potential fluctuations is less meaningful when dealing with monopoles. It can be seen

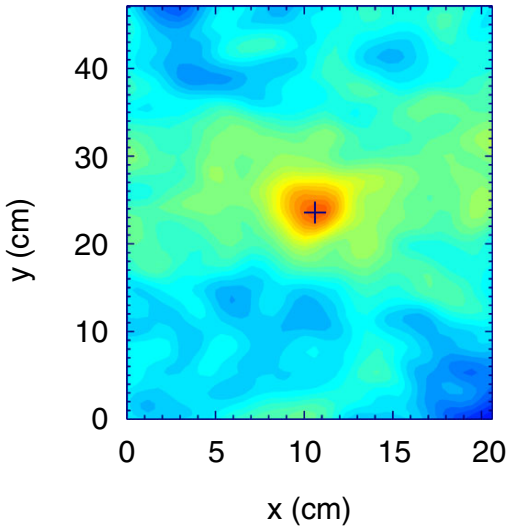

Figure 12. Characteristic structure of a local density maximum, obtained from the simulation by means of conditional averaging.

from the black circle marks (here at the density maxima) that density and potential fluctuations do not coincide. For $\tau = 10$ μs there even is an anti-correlation. This is inconsistent with the drift wave model and has to be further investigated by using a finer grid than the current 1 cm for the probe measurements. On the other hand, as shown in figure 12, the same structure size and monopole character are also found in the simulation data.

5. Summary and discussion

The plasma parameters in TJ-K allow one to study drift-wave turbulence in a regime similar to the one in the edge of fusion plasmas. Other than in high-temperature plasmas, detailed measurements can be carried out in the entire plasma confinement region. The spectra and PDFs found in first experiments are similar to those known from fusion plasmas. A clear turbulent spectrum is present with an exponential decay over more than three decades. The PDFs are more Gaussian for density and potential fluctuations and strongly peaked for transport fluctuations. The size of the fluctuations is in agreement with mixing length estimates and the Boltzmann relation between the density and potential fluctuations is approximately fulfilled.

The experiments are closely co-ordinated with turbulence simulations using the drift-Alfvén turbulence code DALF3, which was written for fusion plasmas. The dimensionless parameters are such that the results should also apply to TJ-K plasmas. Systematic numerical studies have shown that poloidal wavenumber (k) spectra of density and potential fluctuations can serve to reveal the relevant turbulence driving mechanism. Drift-wave transport k spectra have a maximum in the range where the density spectrum already decays exponentially. The density–potential cross phase is in the vicinity of zero. Curvature driven instabilities create a spectrum which is peaked at long wavelengths with cross phases of about $\pi/2$. For the whole range of TJ-K parameters, the drift-wave mechanism is predicted to clearly dominate the interchange mechanism.

Typical spectral parameters of the experimental data are in reasonable agreement with the simulations. Since the probe arrays to measure the poloidal k spectra are not in operation yet, correlation techniques were applied to analyse the spatial structure of the fluctuations. Both direct correlations and conditional averaging are most sensitive to the largest structure. Consequently, the data high-pass filtered at 5 kHz produced structures of the size of about 5 cm which repeat as dipoles. The propagation of the dipole is consistent with the measured potential structure. It is a superposition of $E \times B$ convection in the background electric field and the eddy motion introduced by the potential fluctuations. The dynamics of the dipoles is consistent with a cross phase of about $\pi/2$. They correspond to a quasi-coherent mode in the spectrum at about 8 kHz with a maximum around $\pi/2$ in the cross-phase spectrum.

In order to access smaller scales the data were also filtered at 20 kHz and then processed by conditional averaging. This resulted in monopole structures with a smaller extension. For the cross phases no final conclusions could be drawn yet. They are not constant and even anti-correlated in some cases. However, the structure size and the monopole character was found to be in agreement with the same analysis applied to the simulation data.

Before final conclusions can be drawn, the cross phases at different scales have to be further investigated. Especially the measurement of k spectra is important. A phase of $\pi/2$, as found for the low-frequency structures, would be in variance with the prediction of drift-wave turbulence. However, the experimental situation is more complex. The cross-phase spectrum presented in figure 10 is clearly different from the one in figure 5, which would be typical for pure MHD turbulence. In the latter the cross phase is about $\pi/2$ for all wavelengths while in the experimental one distinct regions with phases of $\pi/2$ are separated by regions with phases close to zero. The regions with phases of $\pi/2$ can be related to a number of modes in the spectrum. The modes might be due to instabilities related to rational ι values or other elements which distinguish a non-ideal device from an idealized numerical plasma. They have a clear MHD character and might also inject energy into the turbulent cascade. However, they appear as peaks on top of a smooth and exponentially decaying turbulence spectrum, which seems to produce small cross phases. For example, around 10 kHz and especially at higher frequencies the phases are close to zero. Hence the dynamics of the turbulence could very well be drift-wave like as predicted by the code. The importance of the modes as an energy source for the background turbulence or for transport has to be investigated further. One attempt will be to create more quiescent plasmas by modifying the magnetic configuration.

From correlation experiments in linear devices [21] and in the fusion SOL [6] phases of typically $\pi/2$ are reported. Since this technique is sensitive to larger modes or events, the same ambiguity as discussed above might also exist. It would also be worthwhile investigating the cross phase at smaller scales in these experiments. On the other hand, there might be a general difference to our experiments, which are carried out in the confinement region. On open field lines the parallel dynamics is determined by the sheath in front of the limiting structures. Hence the sheath and not the parallel resistivity would be responsible for the cross phase and therefore also for the instability.

In conclusion, the first results from comparative studies between measured and simulated turbulence are encouraging to pursue this path to test the physical models used in turbulence codes. The experiment reproduces the major characteristics as predicted by the simulations. More in-depth studies investigating the wavenumber spectra and the cross phases are presently being pursued. The analysis of simulation data with experimental techniques should become a standard approach when new types of analysis tools are proposed.

Acknowledgment

This work is financially supported by the Max-Planck Institut für Plasmaphysik, EURATOM Association.

References

[1] Frisch U 1995 *Turbulence* (New York: Cambridge University Press)
[2] Holmes P, Lumley J L and Berkooz G 1995 *Turbulence, Coherent Structure and Dynamical Systems and Symmetry* (New York: Cambridge University Press)
[3] Liewer C 1985 *Phys. Fluids* **25** 543
[4] Wooton A J *et al* 1990 *Phys. Fluids* B **2** 2879
[5] Endler M *et al* 1995 *Nucl. Fusion* **35** 1307
[6] Bleuel J *et al* 2002 *New J. Phys.* **4** at press
[7] Pedrosa M *et al* 1995 *Plasma Phys. Control. Fusion* **38** 365
[8] Carreras B A *et al* 1999 *Phys. Plasmas* **6** 4615
[9] Carreras B A *et al* 1998 *Phys. Plasmas* **4** 3632
[10] Diamond P H and Kim Y P 1991 *Phys. Fluids* B **3** 1626
[11] Hidalgo C *et al* 2000 *Plasma Phys. Control. Fusion* **42** A153
[12] Diamond P H and Hahm T S 2000 *Phys. Rev. Lett.* **84** 4842
[13] Moyer R A, Tynan G R, Holland C and B M J 2001 *Phys. Rev. Lett.* **87** 135001
[14] Shats M G and Solomon W M 2002 *New J. Phys.* **4** at press
[15] Fonck R J *et al* 1992 *Plasma Phys. Control. Fusion* **34** 1993
[16] Fujisawa A *et al* 1997 *Phys. Rev. Lett.* **79** 1054
[17] Yoshisawa A, Itoh S-I, Itoh K and Nobumitsu Y 2001 *Plasma Phys. Control. Fusion* **43** R1
[18] Garbet X 2001 *Plasma Phys. Control. Fusion* **43** A251
[19] Lin Z *et al* 1998 *Nature* **281** 1835
[20] Kendl A and Wobig H 1999 *Phys. Fluids* **6** 4714
[21] Klinger T *et al* 1997 *Plasma Phys. Control. Fusion* **39** 1
[22] Scott B D 1997 *Plasma Phys. Control. Fusion* **39** 471
[23] Ascasibar E *et al* 1997 *Nucl. Fusion* **37** 851
[24] Krause N *et al* 2002 *Rev. Sci. Instrum.* at press
[25] Lechte C *et al* 2002 *Phys. Plasmas* **9** 2839–46
[26] Niedner S, Scott B D and Stroth U 2002 *Plasma Phys. Control. Fusion* **44** 197
[27] Waltz R E and Boozer A H 1993 *Phys. Fluids* B **5** 2201
[28] Waltz R E, DeBoo J C and Rosenbluth M N 1990 *Phys. Rev. Lett.* **65** 2390
[29] Carbone V, Regnoli G, Martines E and Antoni V 2000 *Phys. Plasmas* **7** 445
[30] Stroth U 1998 *Plasma Phys. Control. Fusion* **40** 9
[31] Pedrosa M A *et al* 1999 *Phys. Rev. Lett.* **82** 3621
[32] Carreras B A *et al* 1996 *Phys. Plasmas* **3** 2664
[33] Sánchez E *et al* 2000 *Phys. Plasmas* **7** 1408
[34] Grulke O, Greiner F, Klinger T and Piel A 2001 *Plasma Phys. Control. Fusion* **43** 525
[35] Thomsen H *et al* 2002 *Phys. Plasmas*